http://dx.doi.org/10.5935/0103-5053.20130025

*J. Braz. Chem. Soc.*, Vol. 24, No. 2, 191-200, 2013.
Printed in Brazil - ©2013 Sociedade Brasileira de Química
0103 - 5053 $6.00+0.00

Article

# Metal Nanostructures with Magnetic and Biodegradable Properties for Medical Applications

*Giacomo Ruggeri,*[a] Vera L. Covolan,[a] Marco Bernabò,[a] Li M. Li,[b] Leonardo F. Valadares,[c] Carlos A. P. Leite[c] and Fernando Galembeck[c]*

[a]*Department of Chemistry and Industrial Chemistry, University of Pisa, Via Risorgimento, 35, 56126, Pisa, Italy*

[b]*Neuroimaging Laboratory, Faculty of Medical Sciences, University of Campinas, CP 6111, 13083-970 Campinas-SP, Brazil*

[c]*Institute of Chemistry, University of Campinas, CP 6154, 13083-970 Campinas-SP, Brazil*

Nanopartículas de Au (AuNP) foram sintetizadas por redução do $HAuCl_4$ com $NaBH_4$ ou ácido l-ascórbico, tendo sido estabilizadas por cisteína, cisteamina e PEG–SH. Com AuNPs, preparou-se um material nanocompósito através da precipitação de soluções acetônicas de ácido poliláctico (PLA), em dispersões aquosas de AuNPs, com obtenção de PLAs completamente impregnados por AuNPs. Nanopartículas de óxido de ferro superparamagnéticas (SPION) modificadas com Au na superfície (SPION@Au NP) foram sintetizadas. SPIONs foram sintetizadas usando-se oleato de ferro como precursor ou pela co-precipitação dos cloretos férrico e ferroso em solução alcalina, com posterior recobrimento das SPION por uma camada de ouro. Os produtos obtidos foram caracterizados por espectroscopia UV-Vis, microscopia de transmissão eletrônica com mapeamento elementar espectroscópico (ESI/TEM) e por análise termogravimétrica (TGA). Em particular, os produtos magnéticos foram testados em um aparelho de ressonância magnética por imagem (MRI) de alto campo clínico. Os resultados obtidos indicaram sua promissora utilização como meios de contraste em análises por MRI.

Gold nanoparticles (AuNPs) were synthesized by reduction of $HAuCl_4$ with $NaBH_4$ or l-ascorbic acid and they were stabilized with cysteine, cysteamine and a thiol-capped PEG. A nanocomposite was prepared by the addition of polylactic acid (PLA) acetone solutions to aqueous AuNP dispersions, resulting in PLAs enclosing AuNPs. Superparamagnetic iron oxide nanoparticles (SPION) modified with Au on the surface (SPION@Au NP) were synthesized. SPIONs were prepared by using iron-oleate as a precursor or by co-precipitation of ferrous and ferric chlorides in alkaline solution and, then used for seed-mediated growth of gold layers on their surfaces. The various nanoparticles were characterized by using UV-Vis spectroscopy, electron spectroscopy imaging/transmission electron microscopy (ESI/TEM) and by thermogravimetric analysis (TGA). The magnetic products were tested in a magnetic resonance imaging (MRI) scanner of high clinical field with results that indicate their promising utilization as contrast agents for MRI analysis.

**Keywords:** gold nanoparticles, poly(lactic acid) (PLA), biocompatibility, biocompatible polymer, stabilizers

## Introduction

Metal nanoparticles have been developed in a multitude of types and used as functional elements in composite materials, in a variety of applications. With the objective to enhance the performance of many materials, nanoparticles in their composition improving them, synergistically, both useful functionality and mechanical integrity. Systems with synergistic properties as the polymer/nanoparticles composites are formulated so as to form the nanoparticles within a polymer matrix by reaction of a precursor salt or complex[1,2] or to introduce them by coprecipitation or melt mixing.[3,4] Aliphatic polyesters had an increasing employment in the preparation of this type of

*e-mail: grugge@dcci.unipi.it

nanocomposites because they are biodegradable materials of great importance for the fabrication of biomedical products. Among the aliphatic polyesters, poly(lactic acid) (PLA) is considered as the most significant material due to its excellent biodegradability and biocompatibility. New composites based on this polymer have been prepared with layered silicates, layered titanates, carbon nanotubes, magnetite, maghemite, silver and gold nanoparticles.[5]

In polymer nanocomposite preparations, when the nanoparticles interact with the host matrix, mechanical properties, barrier effect, thermal stability, crystallization rate, degradation rate and melt strength are often enhanced. Moreover, the polymer matrix can act as particle stabilizer, preventing its aggregation.[6] The advantages of using polymers as stabilizers for gold nanoparticles are not only the enhancement of their long-term stability, adjustment of the solubility and amphiphilicity, but also their functionalization with polymers to achieve higher and tunable surface-density of shell/brush morphology and to tailor its properties, beyond promoting their compatibility and processibility.[7]

Another approach to improve the characteristics of materials based on metal nanoparticles is to build in synergies. Nanoparticles with controlled dimension and structure with modulated optical and magnetic properties can be used in magnetic resonance imaging (MRI) or in cancer thermal therapy. Core-shell particles with a magnetic core and a functional shell can be used for both diagnostic and therapeutic purposes. The magnetic core of the nanoparticles is useful for MRI analyses and their shell can support biologically active species or drugs for biomedical applications.[8] The efficacy of MRI is strongly related to the contrast agents employed to increase the magnetic signal generated inside the living tissue and, the need to use non-toxic contrast agents stimulated the development of new biocompatible agents with enhanced magnetic properties. Previous work has already exploited the magnetic properties of superparamagnetic iron oxide nanoparticles (SPION) with the chemical properties offered by biologically functionalized gold nanoparticles (AuNPs).[9-11]

AuNPs are stable metal nanoparticles that present fascinating aspects such as size-related electronic and optical properties (quantum size effect) and multiple assembly types.[12] These particles have interesting chemical and physical properties, specially concerning the UV-Vis absorption, fluorescence emission, electrochemistry and magnetic properties. It was recently found that dispersed AuNPs capped with thiol groups exhibit ferromagnetic behavior at room temperature, despite the diamagnetic character of bulk Au. These NPs, when embedded in a polyethylene matrix preserve the surprising magnetic properties induced at the nanoscale.[13]

AuNPs for biomedical applications could be considered as advantageous in respect to other metal nanoparticles due to its inert nature, extreme resistance to oxidation and considerable biocompatibility and because their surface charge can be easily modified in order to favor their interaction with biological entities. In fact, proteins spontaneously adsorb on gold surface under slightly basic conditions relative to the isoeletric point.[14] Particularly, plasma proteins and salts in blood nonspecifically adsorb on the surface of bare nanoparticles, forming large aggregates that are rapidly cleared from the bloodstream due to the uptake by the reticular endothelial system (RES), including macrophages in the liver and spleen. Thus, there is a limitation to the direct use of AuNPs *in vivo*, in spite of their biocompatible nature. To use AuNPs *in vivo* for a long retention time avoiding the action of RES, their surfaces must be modified with antibiofouling agents, such as polyethylene glycol (PEG)[15] and more stable bonds can be created by self-assembling molecules with thiol groups on gold surfaces.[14]

Motivated by the well-known properties of PLA and by the interesting AuNP properties, both attractive materials for biomedical applications, our group started a study on the interaction of PLA with AuNP functionalized with molecules containing thiol (–SH) and amine ($–NH_2$) groups. For this purpose, PLA acetone solution was precipitated in aqueous dispersions of AuNP functionalized with cysteine, cysteamine and a thiol-capped polyethylene glycol. Moreover, based on our laboratory expertise in the preparation of metal-based nanostructures with modulated optical[16] and magnetic properties,[13] it was investigated different routes of synthesis of SPION nanoparticles modified by Au on their surface. It was prepared SPION starting from the precursor iron-oleate complex, according to the literature[17] and coated it with gold to obtain a nanostructured material with magnetic properties and amenable to bio-conjugation. Our methodology was also based on the seed-mediated growth of the gold layer on SPION surfaces using SPION previously prepared by co-precipitation of ferrous and ferric chlorides in alkaline solution.

## Experimental

### Materials

Poly(d,l-lactic acid) of MW ca. 6,000-16,000 was purchased from Polysciences Europe. L-cysteine hydrochloride monohydrate and *o*-[2-(3-mercaptopropionylamino)ethyl]-*o*'-methylpolyethylene glycol 5,000 (PEG–SH) were

purchased from Fluka, whereas gold(III) chloride trihydrate, l-cysteine hydrochloride monohydrate, iron(II) chloride tetrahydrate puriss. p.a. ≥ 99.0% (RT), iron(III) chloride anhydrous (powder, 99.99+), sodium citrate dehydrate, cysteamine, cysteine, *o*-[2-(3-mercaptopropionylamino) ethyl]-*o*'-methylpolyethylene glycol 5,000, oleic acid, 1-octadecanol and triethylamine were purchased from Sigma-Aldrich.

## Methods

### Preparation of AuNPs

AuNPs were obtained from an aqueous $HAuCl_4$ solution by the reduction of $Au^{3+}$ to $Au^0$ with $NaBH_4$ by the well-known method described by Brust *et al.*[18] The preparation of AuNPs was carried out by using l-cysteine hydrochloride monohydrate, cysteamine, *o*-[2-(3-mercaptopropionylamino)ethyl]-*o*'-methyl-polyethylene glycol 5,000 without further purifications. Typically, $HAuCl_4$ aqueous solution was mixed with cysteine, cysteamine and cysteamine/PEG–SH aqueous solution under magnetic stirring for 15 min; then an aqueous solution of $NaBH_4$ was added drop by drop at room temperature and left to react for 2 h.

### Preparation of PLA@Au NPs

For the preparation of PLA@Au NP, a PLA acetone solution was precipitated in an aqueous medium containing AuNP previously prepared. For this purpose, two PLAs with different molecular weight were used: a commercial PLA with MW 6,000-16,000 (PLA6) and a PLA with MW 1,000-1,500 (PLA1) that was synthesized in our laboratory as reported in the literature.[19]

Typical preparation: 15 mg of PLA were dissolved in 10 mL of acetone and left under stirring for 1 h; this mixture was precipitated in 25 mL of deionized water and then it was centrifuged; the supernatant was eliminated and the polymer was diluted in 50 mL acetone then, this solution was separated in 3 portions of 15 mL to be used successively. $HAuCl_4$ and $NaBH_4$ were dissolved in 25 mL of water in the presence of cysteine, or cysteamine and/or PEG–SH for the preparation of AuNPs. The PLA acetone solution (15 mL) was added dropwise to the AuNPs aqueous dispersion and then left under magnetic stirring for 2 h. All preparations were purified by dialysis in Milli-Q water and each suspension was collected in a Spectra/Por Molecularporous Membrane (Spectra/Por CE Cellulose Ester, Membrane MWCO:5,000, flat width of 16 mm, diameter of 10 mm, volume *per* length of 0.81 mL $cm^{-1}$) and dialyzed during 3 days changing the dialysis medium 2 times *per* day.

Formulations: in the preparation of Pla1-AuCys and Pla6-AuCys, $HAuCl_4$ (0.25 mmol), $NaBH_4$ (0.2 mmol) and cysteine (0.375 mmol) were used in the molar ratio 1/0.8/1.5. In the preparation of Pla1-AuCysAm and Pla6-AuCysAm, $HAuCl_4$ (0.25 mmol), $NaBH_4$ (0.2 mmol) and cysteamine (0.375 mmol) were used in the molar ratio 1/0.8/1.5. In the preparation of Pla1-AuCysAm-PEG and Pla6-AuCysAm-PEG, $HAuCl_4$ (0.25 mmol), $NaBH_4$ (0.2 mmol), cysteamine (0.187 mmol) and PEG–SH (0.187 mmol) were used in the molar ratio 1/0.8/0.75/0.75.

Pla6-AuCysAm-PEG sample formulation: the formulation of the Pla6-AuCysAm-PEG sample is described in detail in Table 1, referring to the weight and volume of the used components.

**Table 1.** Formulation of the PLA6-AuCysAm-PEG sample

| Component | Formulation |
|---|---|
| PLA6 / mg | 5.6 |
| Acetone / mL | 5.0 |
| $HAuCl_3$ / mg | 1.0 (of which Au = 0.5) |
| $NaBH_4$ / mg | 0.1 |
| Cysteamine / mg | 0.1 |
| PEG-SH / mg | 9.4 |
| $H_2O$ / mL | 100 |

### Preparation of SPION

Two different methods were used for the preparation of SPION: Mag-1 sample was prepared starting from iron-oleate complex as precursor, whereas Mag-2 sample was obtained by co-precipitation of ferric and ferrous iron salts in alkaline medium.

Mag-1: $FeCl_3.6H_2O$ and oleic acid (molar ratio 1:3) were reacted by mixing the following two solutions, (*i*) 5 mmol of $FeCl_3.6H_2O$ in 15 mL of methanol plus 15 mmol of oleic acid and (*ii*) 0.8 g of NaOH in 20 mL of methanol. The NaOH solution was added to the $FeCl_3.6H_2O$ solution under magnetic stirring and, the formation of brown precipitate, ferric oleate complex, was observed which was filtered and dried under vacuum. The obtained ferric oleate was solubilized in 5 g of 1-octadecanol and it was used as stock solution. For the preparation of the Mag-1 sample, all the reagents were heated previously in order to melt them. 3 mL of the ferric oleate solution, 3 mL of 1-octadecanol and 0.5 mL of oleic acid were added in a glass reactor in a sand bath at 320 °C for 30-40 min.; after cooling at room temperature, the reaction product was purified by washings with small portions of warm ethanol at 60-70 °C. The magnetic nanoparticles were collected by a magnet and, successively, washed with another portion of

warm ethanol. The washings were repeated until complete elimination of the excess of oleic acid from de magnetite.

Mag-2: $FeCl_2.4H_2O$ and $FeCl_3$ (molar ratio $Fe^{2+}$/ $Fe^{3+}$ = 1:2) dissolved in 20 mL of Milli-Q degased water were reacted at room temperature, under $N_2$ flux and magnetic stirring. The pH value of the solution initially acid was adjusted to 11 by the addition of a NaOH solution and the formation of the magnetite was observed by decantation of a dark precipitate. The reaction was maintained under $N_2$ flux for 2 h then, the precipitate was centrifuged at 3500 rpm for 5 min, collected and dried under vacuum without any washing.

### Preparation of SPION@AuNP

In the preparation of SPION@Au nanoparticles, the SPION Mag-2 sample was used as seed to be covered by gold. The reaction was based on the reduction of the $Au^{3+}$ to $Au^0$ in presence of SPION by using a $HAuCl_4$ solution and different reducing agents. The following samples were prepared, (*i*) SPION@Au-A: 10 mg of Mag-2 were dispersed in 2 mL of water and the pH value was adjusted to 2 with a diluted HCl solution then, to this dispersion, 0.04 mmol of $HAuCl_4$ and 0.2 mmol of sodium citrate were added, and the Au was reduced by the addition of 0.032 mmol of $NaBH_4$; (*ii*) SPION@Au-B: 10 mg of Mag-2 were dispersed in 2 mL of water and the pH value was adjusted to 2 with a diluted HCl solution, then to this dispersion 0.04 mmol of $HAuCl_4$ and 0.2 mmol of sodium citrate were added, and the Au was reduced by the addition of 0.032 mmol of ascorbic acid.

### Apparatus and analysis

UV-Vis spectra of AuNP were recorded in water suspension by using a Perkin-Elmer Lambda 20 spectrometer.

Transmission electron microscopy (TEM) and elemental spectroscopy imaging (ESI): bright field pictures and the elemental distribution within nanoparticles were obtained using a Carl Zeiss CEM-902 transmission electron microscope, equipped with a Castaing-Henry-Ottensmeyer energy filter spectrometer within the column. When the electron beam passes through the sample, interaction with electrons with different elements results in characteristic energy losses. A magnetic prism-mirror system deflects electrons with different energies to different angles, so that, only electrons with a well-defined energy are selected. If elastic electrons only are chosen (DE ca. 0 eV), a transmission image with reduced chromatic aberration is obtained. When monochromatic inelastic scattered electrons are selected, electron microscopic images are formed, in which contrast is dependent on the local concentration fluctuations of a particular chosen element. Clear areas correspond to element-rich domains. Other experimental details regarding TEM are presented elsewhere.[7]

The particle mean size and particle size distribution were calculated by using the public domain Image Tool 3.00 version image analyzer program.[20]

Thermogravimetric analysis was carried out by a Mettler Toledo TGA/SDTA 851 working under nitrogen flow (50 mL $min^{-1}$). The sample was analyzed in the range of 25-700 °C with a scanning speed of 10 °C $min^{-1}$.

The MRI scan of nanoparticle water suspensions was collected by using a scanner of high clinical field of 2 T (model Elscint, Prestige, Haifa, Israel), and for the evaluation of the data protocols with weighable, sequences in T2 were utilized: spin-echo T2, fast-spin-echo T2, gradient-recall-echo T2. The images were obtained in the format DICOM and processed by using the software MaZda[21] and the images were analyzed by comparing their gray tonalities with that of pure water.

## Results and Discussion

For the preparation of PLA@Au NP, three sets of AuNP were prepared using different stabilizing agents (cysteine, cysteamine and PEG–SH).

### Gold nanoparticles

AuNPs were prepared in the presence of molecules containing thiol (–SH) and amine ($–NH_2$) groups as cysteine, cysteamine and a thiol-capped PEG in order to avoid the nanoparticle aggregation especially in aqueous solution. All aqueous dispersions of AuNP samples before dialysis were homogeneous, with color ranging from red-wine to greyish blue, typical of finely-dispersed gold nanoparticles.[22] In order to verify if and how the used stabilizing agents covered the AuNPs, TEM images with elemental maps for S, N, O and C elements were acquired (Figure 1).

In Figure 1, the elemental maps of N and S confirm that AuNPs are coated with cysteamine. It is known that AuNPs with different shapes and sizes can be obtained depending on the synthetic method used[23] and equilibrium shape can be achieved under certain experimental growth conditions.[24] In our observation of the TEM images, the shape of AuNPs tends to be hexagonal, typical of the fcc structure.

### PLA@Au nanoparticles

The preparation of PLA containing dispersed AuNPs was carried out taking into account the biodegradability

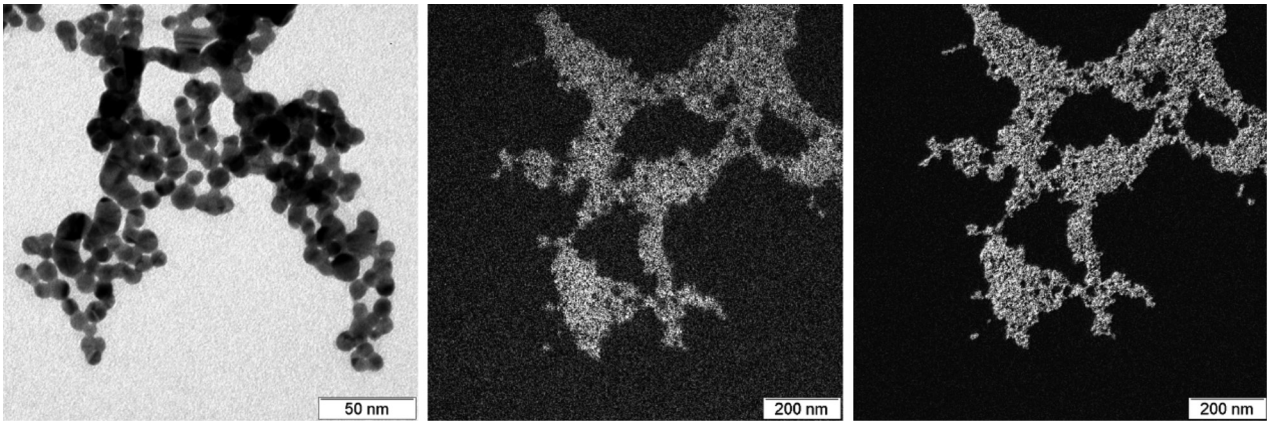


**Figure 1.** TEM micrographs and elemental maps of the sample AuNP stabilized with cysteamine: bright field image on the left, N elemental map at the center and S elemental map on the right.

of this polymer that could contribute to extend the AuNP retention time in the body. Thi is due to the fact that their biodegradation time can switch from days to weeks. The biodegradability of PLA and its copolymers depends on various factors: water permeability or solubility, chemical composition, porosity and polymer molecular weight, among others, but in this work, the biodegradation time of PLA@Au NPs was not investigated. The interaction of PLA with AuNP was investigated by means of UV-Vis, ESI-TEM and TGA analyses.

In the preparations of PLA@Au NPs, different stabilizers and PLA samples were used. The use of functionalized PLA or its modification by thiol groups to anchor AuNPs was previously reported in the literature.[15,25-27] In this work, it was used two unmodified PLA samples (one of lower molecular weight (PLA1, MW 1,500) and another of higher molecular weight (PLA6, MW 6,000-16,000)) relying on the fact that the stabilizers used to coat nanoparticles would guarantee a sufficient interaction with the polymer to allow their incorporation.

The procedure of PLA@Au NPs preparation is schematically illustrated in the scheme shown in Figure 2.

The UV-Vis spectra of the functionalized AuNPs and PLA@Au NPs (see Figure S1 in the Supplementary Information (SI) section), recorded before the dialysis of the samples, show the typical absorption band in the visible region due to surface plasmon resonance (SPR). SPR of an AuNP reference sample with a size distribution within 3-4 nm has the $\lambda_{max}$ at 535 nm, whereas AuNPs stabilized by cysteine, cysteamine and those stabilized with PEG–SH

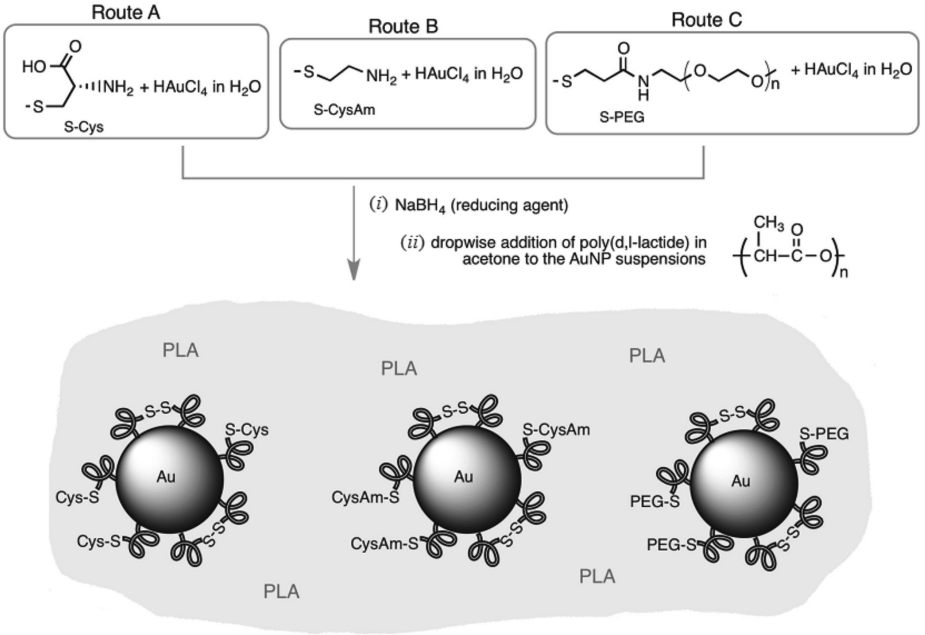


**Figure 2.** Schematic representation of PLA@Au NP preparations. Three different AuNPs were used: (A) AuNP functionalized with cysteine, (B) AuNP functionalized with cysteamine and (C) AuNP functionalized with PEG-SH and cysteamine.

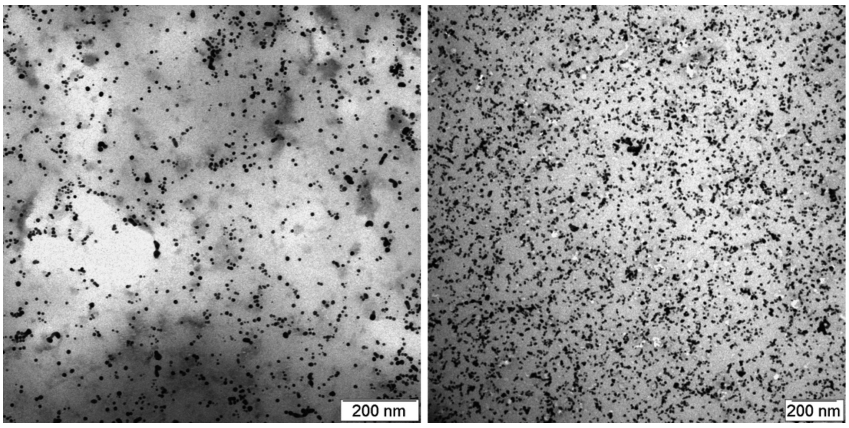


**Figure 3.** TEM micrographs of AuCysAmNP in PLA1 (left) and in PLA6 (right).

embedded in PLA have $\lambda_{max}$ values between 530-545 nm indicating that they are larger perhaps due to the presence of the coating agents and PLA. In fact, for spherical gold nanoparticles, the plasmon band maximum generally falls between 520 and 530 nm.[28] By varying the particle shape, size and spacing between AuNPs, the spectral position of the SPR $\lambda_{max}$ changes and, accordingly, it is possible to tune it within a wide range of wavelengths. The position of SPR $\lambda_{max}$ of gold nanospheres depends on the surrounding dielectric constant, thus the use of different solvents or the adsorption of a capping agent on the nanoparticle surface may result in a slight variation for the SPR $\lambda_{max}$ position. The UV-Vis spectra of AuNPs gave us an indication that the nanoparticles studied in this work could be spherical but not necessarily very homogeneously dispersed in the medium. Mixed cysteamine and PEG–SH were the best stabilizers for AuNPs whereas those prepared with only cysteamine or cysteine produced agglomerates that easily sedimented.

When AuNPs interacted with PLA, the resulting nanoparticles were stable but those produced with PLA6 decanted faster than those prepared with PLA1. This is probably due to the different chain lengths of the macromolecules. After PLA interaction, the samples containing cysteamine had a red-wine color indicating the persistence of smaller gold particles.

After dialysis in Milli-Q water, the AuNPs samples containing PLA formed polymer precipitates, which differ from their corresponding blank dispersions (without PLA). Again, the formulations based on PLA1 produced smaller amounts of precipitates as compared to those based on PLA6. The formulations containing cysteine were greyish blue, whereas the other samples were wine red, typical of smaller gold nanoparticles. TEM images of AuNP stabilized by cysteamine and enclosed in PLA1 or PLA6 matrix can be seen in Figure 3.

From the TEM images, it is possible to verify that AuNPs enclosed in PLA1 were more separated and less concentrated than those incorporated in the PLA6 polymer matrix. As the polymer matrix can act as particle stabilizer,[6] it seems that PLA6 was more effective in the stabilization of AuNPs than PLA1, incorporating a larger amount of nanoparticles *per* volume unit, with less aggregation. The particle mean size and size distribution were calculated by using the Image Tool 3.00 image analyzer program,[20] and graphics similar to PLA1-AuCysAm (Figure 4) were obtained for all samples.

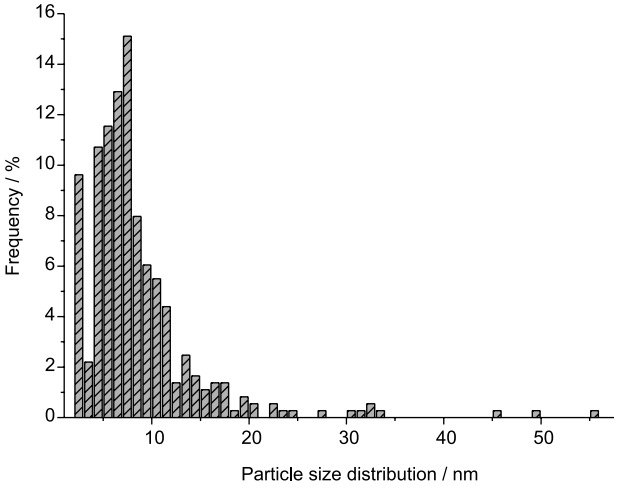


**Figure 4.** Histogram of nanoparticle size distribution of AuNP-CysAm in PLA1.

Table 2 shows the particle mean size of the previously described AuNPs.

**Table 2.** Nanoparticle sizes measured from TEM micrographs (nm)

| Stabilizer | AuNPs | PLA1-AuNPs | PLA6-AuNPs |
|---|---|---|---|
| Cys | 6.5 ± 1.6 | 7.2 ± 2.5 | nd |
| CysAm | 9.8 ± 1.9 | 8.5 ± 6.3 | 8.5 ± 6.7 |
| CysAmPEG | 12.3 ± 10.4 | 11.0 ± 10.0 | 14.5 ± 12.7 |

nd: not determined.

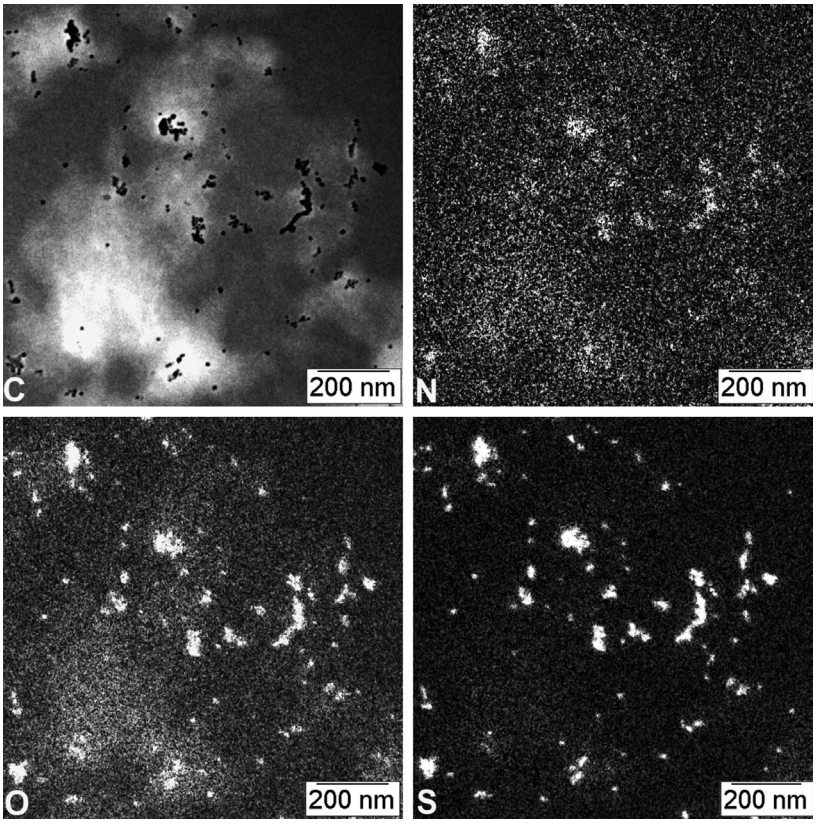


**Figure 5.** TEM elemental maps (C, N, O and S) of the AuNP particles stabilized with cysteamine enclosed in PLA1 matrix.

Particles stabilized with cysteine were the smallest, while those stabilized with a mixture of cysteamine and PEG–SH were the largest. The mixture of stabilizers (cysteamine and PEG–SH) produced always suspensions of nanoparticles with larger dimensions and broad size distribution, in agreement with UV analysis (Figure S1 in the SI section). Despite this fact, AuNPs stabilized by CysAm-PEG were the most stable in water. Despite this fact, the AuNPs stabilized by both, CysAm and PEG, were that more stable in water. PEG-SH seems to have been the main stabilizing agent since AuNPs stabilized by cysteamine produced larger particles that easily decanted.

In this work, it was not our intention to control the particles shape and size, the aim was to verify the interaction of PLA with the coating agents of AuNPs. For this reason, our attention was more directed to the elemental analysis of the samples by ESI-TEM (Figure 5).

In Figure 5, it is possible to see AuNPs as black dots enclosed in the zones of light gray tones of the polymer matrix. The C map confirms the presence of PLA matrix, the O map indicates the presence of PLA diffused in the image but accumulated on the particle surfaces while the S and N maps confirm the interaction of cysteamine with AuNPs.

The PLA6-AuCysAm sample presented the same morphological features of PLA1-AuCysAm sample but PLA had also the morphology of flattened particles (Figure 6).

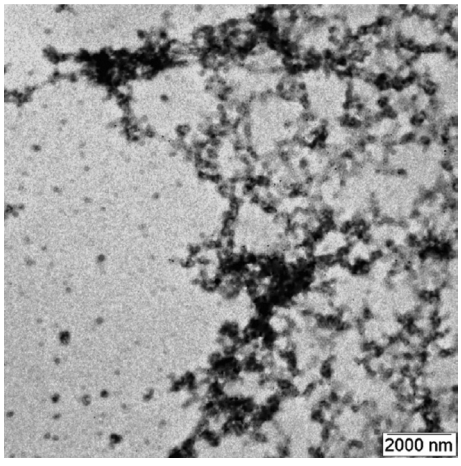


**Figure 6.** TEM micrograph of the PLA6-AuCysAm sample with PLA flattened particles.

This morphology is due the fact that PLA is a soft polymer of low Tg (about 60-65 °C) and under the TEM microscopy operating set-up, the polymer is easily deformed during image acquisition.

The PLA6-AuCysAmPEG–SH sample, which contains more components, was analyzed by thermogravimetric analysis (details and Figure S2 are in the SI section). By

subtracting the weight loss attributed to the cysteamine and PEG–SH, it was verified that the amount of $Au^{+3}$ used in the synthesis was totally reduced to $Au^0$. By considering the PLA6-AuCysAmPEG–SH sample as a composite material, an important influence of the AuNPs in the thermal stability of this composite can be verified by comparing the degradation temperature of the pristine PLA6 and that of the PLA6-AuCysAmPEG–SH sample. The onset of PLA6 calculated from TGA analysis was 261 °C, whereas that of the PLA6-AuCysAmPEG–SH sample was 313 °C. The 52 °C higher degradation temperature of the composite material can be interpreted as positive effect of AuNPs stabilized by PEG–SH and cysteamine on the thermal stability of PLA6.

### SPION@Au nanoparticles

The preparation of SPION was carried out by using two different methods, using an iron-oleate complex (Mag-1 sample) or the co-precipitation of ferrous and ferric chloride in alkaline solution (Mag-2 sample), followed by seed-mediated growth of a gold layer. The Mag-1 sample was imaged by TEM as shown in Figure 7.

SPION presented a good dispersion without aggregation and particle mean sizes in the 5-10 nm range. Despite the suitable morphology of this SPION sample, the method to prepare them as well as the products used in their preparation are not easily manipulated. In fact, the SPION preparation based on the utilization of the precursor iron-oleate complex is too long and requires handling the products at high temperature. Then, for the preparation of SPION@Au NPs, a simpler route was chosen: co-precipitation of ferrous and ferric chloride in alkaline solution,[29] followed by seed-mediated growth of the gold shell by reduction of the gold precursor ($HAuCl_4$) with $NaBH_4$ and L-ascorbic acid, respectively, in presence of sodium citrate as stabilizing agent.

The coverage of SPION particles with a layer of Au particles with nanometric dimensions was evidenced by UV-Vis spectroscopy analyses (Figure S3 in the SI section) that show the typical surface plasmon band of nanostructured gold particles between 500 to 600 nm. The presence of Fe and Au in the particles was confirmed by TEM elemental mapping (Figure 8). Both samples obtained by reduction with $NaBH_4$ and l-ascorbic acid showed a similar morphology.

The evaluation of the SPION@Au sample as contrast agent was made based on the measurements of the transversal relaxation time T2 through the application of a radio frequency pulsed single and double fast spin-echo sequences (FSE-T2), by using a typical clinical scanner for magnetic resonance imaging (MRI), operating with a magnetic field of 2 T, according to our previous protocols.[30] The responses of the two samples exposed to the T2 weighted FSE sequences were elaborated by the instrument using the signal of pure water as reference and then translated into MR images with high contrast. The SPION@Au-A and SPION@Au-B samples showed grey signal when compared with the bright pure water standard, as shown in Figure 9.

This promising result was achieved using very dilute nanoparticles suspensions and it confirms the possibility of using these nanoparticles as contrast agents in clinical MRI analysis, with the interesting possibility to be used also as a therapeutic product by using Au sites for bio-conjugation of drugs used in chemotherapy. Moreover, this system could also be used in thermal therapy to destroy cancer cells.

## Conclusions

PLA containing nanostructured gold particles was obtained by co-precipitation of the polymer from acetone

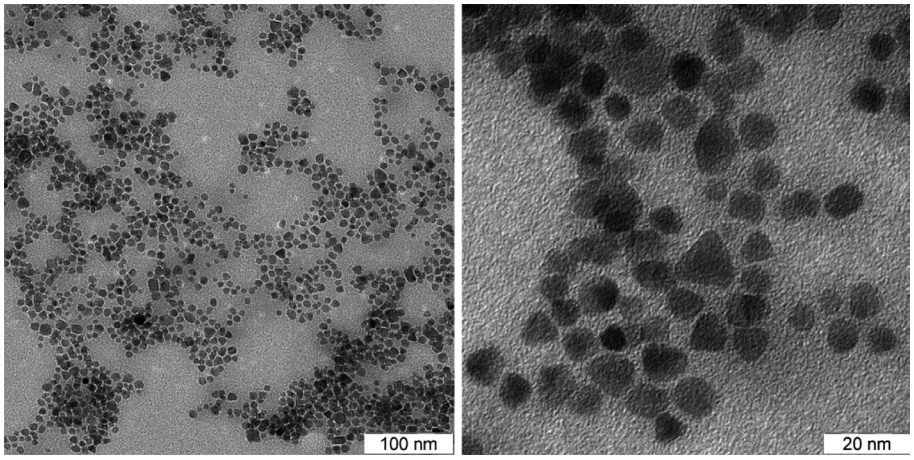


**Figure 7.** TEM micrographs from Mag-1 sample.

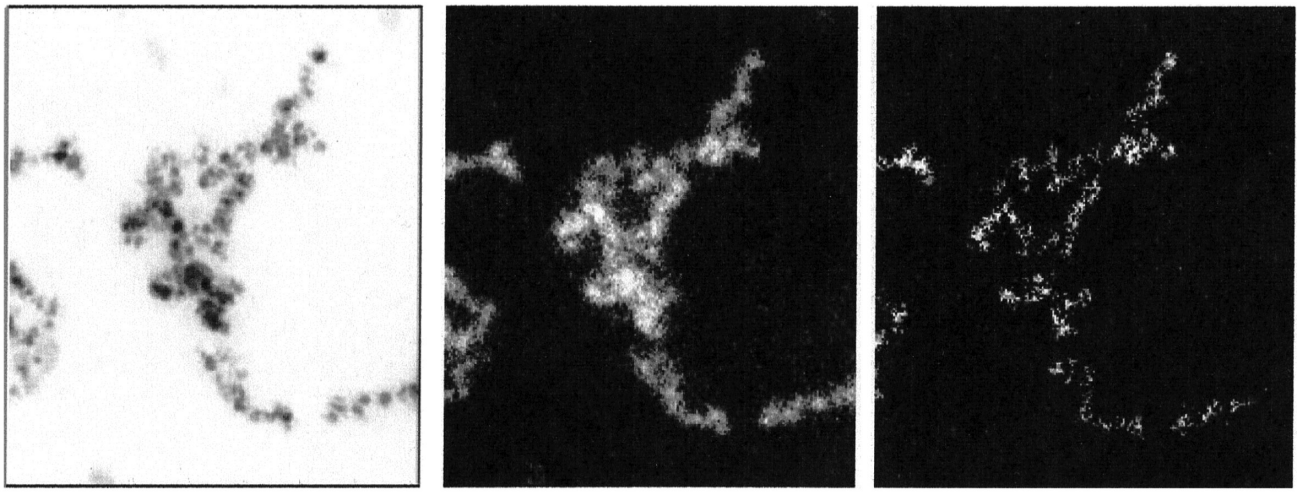

**Figure 8.** Details of the images obtained by TEM elemental analysis of the SPION@Au-B sample: bright field (left), Au map (center) and Fe map (right).

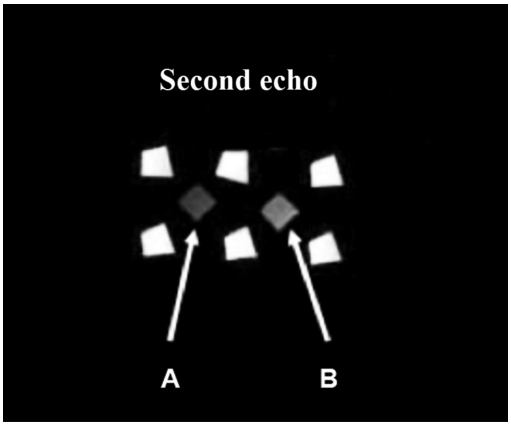


**Figure 9.** Second FSE MR images of the (A) SPION@Au-A and (B) SPION@Au-B.

solution within aqueous dispersions of gold nanoparticles, which are fully incorporated to the PLA matrix. The use of different biocompatible molecules, such as cysteine, cysteamine and PEG–SH in the formation of AuNPs in aqueous dispersion has allowed to compare their effect on nanoparticle stabilization. The use of a mixture of cysteamine and PEG–SH produced the more stable suspensions, while cysteine produced smaller particles. Besides, the introduction of AuNPs in the polymer matrix conferred to PLA higher thermal stability.

The interaction of AuNPs in the PLA matrix were confirmed by TEM elemental mapping. S, N, O and C from cysteamine, cysteine and PEG–SH were observed on the particles surface by electron spectroscopy imaging in the transmission microscope (ESI-TEM). The results show that a PLA without particular chemical modifications is still a good polymer matrix to embed AuNPs when they are coated with cysteine, cysteamine and/or PEG–SH.

By taking into account the need of a biocompatible or biomimetic coating of the AuNPs for *in vivo* applications, the diverse formulations of AuNPs embedded in PLA described in this work can be considered as a promising starting point to prepare new nanoparticle formulations for biomedical applications.

SPIONs prepared by two different methods produced 5-10 nm nanoparticles that were successfully coated with gold producing SPION@Au nanostructures verified by ESI analysis. MRI analysis demonstrated the presence of an effective magnetic signal for the tested samples.

SPION@Au seems to be very interesting for biomedical applications thanks to their intrinsic synergistic properties. Indeed, it is possible to use them either as a diagnostic tool for MRI analysis while they can also be modified by attachment of biological species or drugs on the biocompatible gold surface.

## Supplementary Information

Supplementary data are available free of charge at http://jbcs.sbq.org.br as PDF file.

## Acknowledgment

This work was supported by FAPESP (Fundação de Apoio à Pesquisa do Estado de São Paulo, Brazil, Project 06-53498-2), by 'Azioni di Sostegno alla Cooperazione Accademica Internazionale 2011-2012' in the frame of the Cooperation Agreement between University of Pisa and University of Campinas and by CNPq and Fapesp under the INCT program.

### References

1. Scalzullo, S.; Mondal, K.; Witcomb, M.; Deshmukh, A.; Scurrell, M.; Mallick, K.; *Nanotechnology* **2008**, *19*, 075708.

2. Mallick, K.; Witcomb, M. J.; Scurrell, M. S.; *Eur. Polym. J.* **2006**, *42*, 670.
3. Hsu, S. H.; Chou, C. W.; Tseng, S. M.; *Macromol. Mat. Eng.* **2004**, *289*, 1096.
4. Hirai, T.; Watanabe, T.; Komasawa, I.; *J. Phys. Chem. B* **2000**, *104*, 1089.
5. Yang, K. K.; Wang, X. L.; Wang, Y. Z.; *J. Ind. Eng. Chem.* **2007**, *13*, 485.
6. Shan, J.; Tenhu, H.; *Chem. Commun.* **2007**, *44*, 4580.
7. Heilmann, A.; *Polymer Films with Embedded Metal Nanoparticles*, Springer Series in Materials Science; Springer: Berlin, Germany, 2003.
8. Park, H. Y.; Schadt, M. J.; Wang, L; Lim, I. S.; Njoki, P. N.; Kim, S. H.; Jang, M. Y.; Luo, J.; Zhong, C. J.; *Langmuir* **2007**, *23*, 9050.
9. Reddy, A. N.; Anjaneyulu, K.; Basak, P.; Rao, N. M.; Manorama, S. V.; *ChemPlusChem* **2012**, *77*, 284.
10. Tsai, J. K.; Wu, T. L.; Chao, S. M.; Lam, K. T.; Meen, T. H.; Huang, C. J.; Chen, W. R.; *Ferroelectrics* **2011**, *421*,43.
11. Na, H. B.; Song, I. C.; Hyeon, T.; *Adv. Mater.* **2009**, *21*, 2133.
12. Kreibig, U.; Vollmer, M.; *Optical Properties of Metal Clusters*; Sprinter-Verlag: Berlin, Germany, 1995.
13. de la Venta, J.; Pucci, A.; Pinel, E. F.; García, M. A.; Fernandez, C. J.; Crespo, P.; Mazzoldi, P.; Ruggeri, G.; Hernando, A.; *Adv. Mater.* **2007**, *19*, 875.
14. Longmire, M.; Choyke, P. L.; Kobayashi, H.; *Nanomedicine* **2008**, *3*, 703.
15. Kim, D.; Park, S.; Lee, J. H.; Jeong, Y. Y.; Jon, S.; *J. Am. Chem. Soc.* **2007**, *129*, 7661.
16. Pucci, A.; Bernabò, M.; Elvati, P.; Meza, L. I.; Galembeck, F.; Leite, C. A. P.; Tirelli, N.; Ruggeri, G.; *J. Mater. Chem.* **2006**, *16*, 1058.
17. Park, J.; An, K.; Hwang, Y.; Park, J. G.; Noh, H. J.; Kim, J. Y.; Park, J. H.; Hwang, N. M.; Hyeon, T.; *Nat. Mater.* **2004**, *12*, 891.
18. Brust, M.; Walker, M.; Bethell, D.; Schiffrin, D. J.; Whyman, R.; *J. Chem. Soc., Chem. Commun.*1994, 801.
19. Kowalski, A.; Duda, A.; Penczek, S.; *Macromolecules* **2000**, *33*, 7359.
20. http://compdent.uthscsa.edu/imagetool.asp accessed in November 2012.
21. http://www.eletel.p.lodz.pl/programy/cost/progr_mazda_eng.html accessed in November 2012.
22. Wyrwas, R. B.; Alvarez, M. M.; Khoury, J. T.; Price, R.C.; Schaaff, T. G.; Whetten, R. L.; *Eur. Phys. J. D* **2007**, *43*, 91.
23. Lee J. H.; Kamada, K.; Enomoto, N.; Hojo, J.; *J. Colloid Interface Sci.* **2007**, *316*, 887.
24. Ascencio, J. A.; Pérez, M.; Yacamán, M. J.; *Surf. Sci.* **2000**, *447*, 73.
25. Nobs, L.; Buchegger, F.; Gurny, R.; Allémann, E.; *Int. J. Pharm.* **2003**, *250*, 327.
26. Qiu, H.; Rieger, J.; Gilbert, B.; Jérôme, R.; Jérôme, C.; *Chem. Mater.* **2004**, *16*, 850.
27. Gao, X.; Tao, W.; Lu, W.; Zhang, Q.; Zhang, Y.; Jiang, X.; Fu, S.; *Biomaterials* **2006**, *27*, 3482.
28. Kwon, K.; Lee, K. Y.; Lee, Y. W.; Kim, M.; Heo, J.; Ahn, S. J.; Han, S. W.; *J. Phys. Chem. C* **2007**, *111*, 1161.
29. Kim, D. K.; Mikhaylova, M.; Zhang, Y.; Muhammed, M.; *Chem. Mater.* **2003**, *15*, 1617.
30. Haddad, P. S.; Martins, T. M.; D'Souza-Li, L.; Li, L. M.; Metze, K.; Adam, R. L.; Knobel, M.; Zanchet, D.; *Mater. Sci. Eng. C* **2008**, *28*, 489.

*Submitted: October 25, 2012*
*Published online: December 12, 2012*

**FAPESP has sponsored the publication of this article.**